Available online at www.sciencedirect.com
ScienceDirect
Journal of Hazardous Materials 150 (2008) 679–686
Journal of Hazardous Materials
www.elsevier.com/locate/jhazmat

Imidacloprid oxidation by photo-Fenton reaction

Cristina Segura [a,*], Claudio Zaror [a], Héctor D. Mansilla [b], María Angélica Mondaca [c]

[a] *Departamento de Ingeniería Química, Facultad de Ingeniería, Universidad de Concepción, Correo 3, Casilla 160-C, Concepción, Chile*
[b] *Departamento de Química Orgánica, Facultad de Ciencias Químicas, Universidad de Concepción, Correo 3, Casilla 160-C, Concepción, Chile*
[c] *Departamento de Microbiología, Facultad de Ciencias Biológicas, Universidad de Concepción, Correo 3, Casilla 160-C, Concepción, Chile*

Received 8 March 2007; received in revised form 4 May 2007; accepted 8 May 2007
Available online 13 May 2007

Abstract

This paper presents experimental results on the imidacloprid removal from wastewater using homogeneous photo-Fenton reactions illuminated with black light lamps. Multivariate experimental design was used to identify the effect of initial Fe(II) and H_2O_2 concentrations on process performance. The initial iron concentration played a key role in the process kinetics, whereas hydrogen peroxide concentration directly affected the extent of the oxidation process.

Imidacloprid degradation proceeded via two distinctive kinetics regimes, an initial stage of rapid imidacloprid reduction, followed by a slower oxidation process until complete removal. Under optimal conditions, more than 50% imidacloprid degradation was observed after less than 1 min treatment, and TOC and COD removal up to 65% and 80%, respectively, were measured after all hydrogen peroxide was consumed.

Raw imidacloprid samples presented significant acute toxicity to *Daphnia magna* and genotoxic effects on *Bacillus subtilis* sp. Such toxic effects remained detectable even after significant pesticide removal had been achieved, due to the presence of toxic by-products. Both acute toxicity and genotoxicity disappeared after considerable mineralization resulting in final low molecular weight by-products. Results obtained here confirm that design and operation of photo-Fenton processes should focus on toxicity removal rather than on specific target pollutants.

Keywords: Imidacloprid; Factorial design; Photo-Fenton; Toxicity evaluation

1. Introduction

Water pollution by pesticides used in industry and agriculture constitutes a serious environmental problem due to potential toxicity and bioaccumulation.

In this context, the growing use of imidacloprid, a chloronicotinic insecticide, has raised environments concerns due to its relatively high solubility ($0.58\,g\,L^{-1}$), stability in water and low degradation by photolysis [1–3]. Advanced oxidation processes, such as Fenton (Fe(II)/H_2O_2) and photo-Fenton (Fe(II)/H_2O_2/UV), have already been identified as a potential option to remove pesticides from contaminated water [4–9].

The oxidation power of Fenton reaction is attributed to the generation of hydroxyl radicals during the catalytic decomposition of hydrogen peroxide [10]:

$$Fe^{2+} + H_2O_2 \rightarrow Fe^{3+} + OH^- + HO^\bullet \quad (1)$$

In turn, Fe(III) rapidly reacts with hydrogen peroxide forming Fe(II) [11]:

$$Fe^{3+} + H_2O_2 \Leftrightarrow FeOOH^{2+} + H^+ \quad (2)$$

$$Fe\text{–}OOH^{2+} \rightarrow HO_2^\bullet + Fe^{2+} \quad (3)$$

$$Fe^{3+} + HO_2^\bullet \rightarrow Fe^{2+} + O_2 + H^+ \quad (4)$$

When UV light is added, Fe(III) photo reduction regenerates Fe(II) improving the effectiveness of the process due to the formation of new hydroxyl radicals [12]:

$$Fe(OH)^{2+} + h\nu \rightarrow Fe^{2+} + HO^\bullet \quad (5)$$

Imidacloprid degradation by photo-Fenton and heterogeneous photocatalysis using a solar pilot plant has been reported

* Corresponding author. Tel.: +56412204762; fax: +56412207491.
E-mail address: crsegura@udec.cl (C. Segura).

0304-3894/$ – see front matter © 2007 Elsevier B.V. All rights reserved.
doi:10.1016/j.jhazmat.2007.05.018

[7,13,14]. Up to 95% of mineralization was achieved and the final effluent did not present any acute toxicity to *Daphnia magna*. However, the effect of hydrogen peroxide and iron concentrations on imidacloprid oxidation is not clearly understood. Moreover, no published information exists on possible formation of genotoxic by-products generated as a result of imidacloprid oxidation by photo-Fenton processes. Complete imidacloprid degradation may not lead to full removal of acute toxicity and/or genotoxicity effects. Thus, design and operation of photo-Fenton processes should focus on toxicity removal rather than on specific target pollutants.

In this paper, experimental results are presented on the effect of reagents concentrations on imidacloprid oxidation, and both acute toxicity and genotoxicity removal by photo-Fenton treatment. Central composite factorial experimental design is used here to study the system response. The aim of this work is to determine optimal conditions for imidacloprid removal.

2. Materials and methods

2.1. Reagents

Imidacloprid was extracted from commercial Confidor350® SC (Bayer, Chile), by Soxhlet extraction with methylene chloride (Merck) and dried in vacuum at 40 °C. Analytical grade imidacloprid, purchased from Rielden-de Häen, was used for HPLC analysis. The imidacloprid structure is shown in Fig. 1. Photo-Fenton experiments were carried out using heptahydrated iron sulfate ($FeSO_4{\cdot}7H_2O$) (99.5% w/w, Merck), hexahydrated iron chloride ($FeCl_3{\cdot}6H_2O$) (>98% w/w, Scharlau) and hydrogen peroxide (30% w/w, Merck); sulfuric acid (97–98% w/w, Merck) was used for pH adjustment.

Hydrogen peroxide consumption was monitored using Merckoquant® peroxide analytical test strip (range 0.5–25 y 1–100 mg L^{-1} H_2O_2) (Merck). Ultrapure water (18 μS cm^{-1}), acetonitrile HPLC grade, ortho-phosphoric and di-sodium hydrogen phosphate dodecahydrated (analytical grade, all provided by Merck) were used in HPLC determinations. All solutions were prepared using bi-distilled water.

2.2. Experimental scheme

Fig. 2 shows the experimental system used here. The 2L jacketed Pyrex glass reactor features magnetic stirring, and three 6W Philips black light fluorescent lamps (λ_{max} 365 nm), arranged in parallel to the reactor axis. These lamps are encapsulated in Pyrex glass tubes. The incident light intensity in the reactor, as determined by potassium ferrioxalate, was 5×10^{-6} Einstein s^{-1} [15]. Temperature was kept at 25 ± 1 °C by water circulation through the reactor jacket. Initial imidacloprid concentration was set at 100 mg L^{-1} in all cases, and initial pH was adjusted to 2.8 using 9N sulfuric acid.

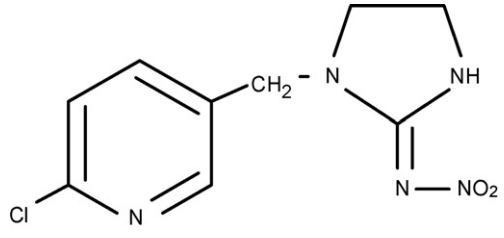

Fig. 1. Imidacloprid structure. [1-(6-Chloro-3-pyridylmethyl)-*N*-nitroimidazolidin-2-ylideneamine].

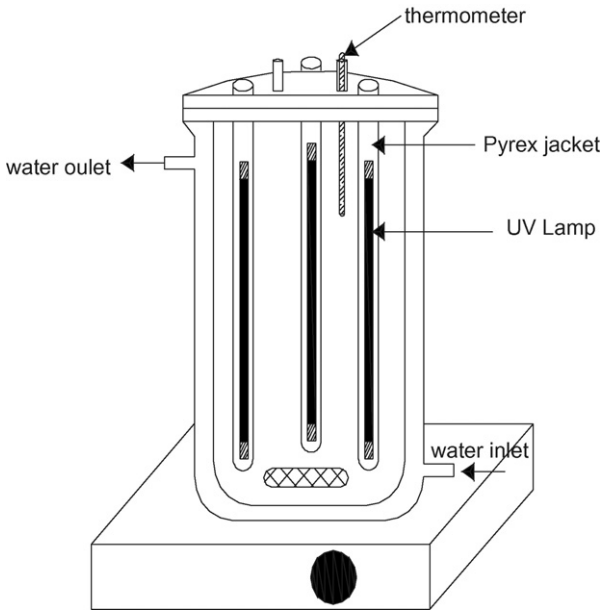

Fig. 2. Experimental set-up of the photoreactor used in the photo-Fenton experiments. Reactor (2 L) with three 6 W Philips black light fluorescent lamps ($I = 5 \times 10^{-6}$ Einstein s^{-1}), operated in batch conditions with controlled temperature.

Typically, $FeSO_4{\cdot}7H_2O$ was added to the reactor to achieve the required initial concentration. Then, lamps were switched on, and a set amount of H_2O_2 was added. Samples were collected at different intervals, placed into test tubes containing 30 μL sodium disulfite 40% w/w to stop the reaction, and then stored at 5 °C for further analysis. Additionally, experiments were conducted using Fe(III) and Fe(II)/Fe(III) mixtures as initial iron sources.

2.3. Analytical methods

Imidacloprid insecticide was assayed using reverse phase HPLC-UV (Merck Hitachi, L-7100 pump, and UV L-7400 detector), equipped with a RP-18e column (Purosfer® Star RP-18e 5 μm, 4.6 mm × 150 mm, Merck). The mobile phase was a mixture of ultrapure water buffered at pH 3 and acetonitrile (75/25 v/v), and run at 1 mL min^{-1}, 20 °C, 20 μL injection volume. Detection was set at 270 nm.

Chemical oxygen demand (COD) was determined by closed reflux colorimetric method [16], previous removal of residual hydrogen peroxide by sodium hydrogen sulphite. In order to prevent hydrogen sulphite presence during COD determinations, a 2 mg L^{-1} H_2O_2 was allowed. A Shimadzu UV-1603 photometer was used to determine absorbance at 585 nm.

Fe(II) concentration was measured by colorimetric determination with 1,10-phenantroline using procedure described by

Table 1
Central composite design of photo-Fenton oxidation of imidacloprid and corresponding results obtained

Experiment	$[H_2O_2]$ (x_1) (mg L^{-1})	[Fe(II)] (x_2) (mg L^{-1})	T_{80} (min)	Y (%)	T_F (min)
1	150 (−1)	15 (−1)	21.0	24.3	70
2	400 (+1)	15 (−1)	23.8	72.6	140
3	150 (−1)	35 (+1)	7.5	20.0	38
4	400 (+1)	35 (+1)	11.0	70.9	102
5	98.25 (−1.414)	25 (0)	16.0	9.5	48
6	451.75 (+1.414)	25 (0)	12.7	76.5	145
7	275 (0)	10.86 (−1.414)	27.5	65.5	97
8	275 (0)	39.14 (+1.414)	5.8	49.4	47
9	275 (0)	25 (0)	12.8	67.3	60
10	275 (0)	25 (0)	11.8	66.0	58
11	275 (0)	25 (0)	11.8	65.1	62

T_{80}: the time required to removal 80% of imidacloprid; Y: total organic carbon (TOC) removal yield; T_F: the time required to achieve total consumption of hydrogen peroxide.

Murov [15]. Total organic carbon (TOC) was determined by direct injection in a Shimadzu TOC-VCPN analyser.

2.4. Toxicity analysis

2.4.1. Acute toxicity

Acute toxicity was assessed by bioassay using *Daphnia magna*, according to procedure describe by standard methods [17,18]. Cultures were conducted under natural light conditions for a period of 16 h and 8 h under darkness, at 20 ± 2 °C, and dissolved oxygen was kept over 80% saturation level. Samples were diluted with distilled water, at different dilutions, and cultures were conducted under batch conditions throughout the test. The mean lethal concentration 50% (LC_{50}) was determined after 24 and 48 h culture.

2.4.2. Bacillus subtilis assay

Preliminary assessment of genotoxicity was carried out using the *Bacillus subtilis* method described by Mazza [19]. This analysis has been widely used as a quantitative measure of the extent of DNA damage due to the presence of a contaminant. Two isogenic *Bacillus subtilis* strains were used here. One strain, the 1652 rec(+), presents the ability to self-repairing any DNA damage and, therefore, the presence of genotoxic pollutants should have no affect on growth. On the other hand, the 1791 rec(−), strain is incapable of repairing any DNA damage and, growth should be significantly affected by genotoxic compounds. Strains were cultured for 24 h at 37 °C, on agar plates containing samples at various dilutions.

DNA damage is expressed as plaque efficiency, i.e. the ratio between the viable bacterial counts in the presence (N) and absence (N_0) of the contaminant. The relative affinity (A) provides a measure of the extent of the contaminant's genotoxic potential, and is estimated as the ratio between the 1791 rec(−) and the 1652 rec(+) strains plaque efficiencies by using the Eq. (5).

$$A = \frac{N/N_0\text{rec}(-)}{N/N_0\text{rec}(+)} \quad (5)$$

Samples featuring relative affinities below 0.9 could be considered genotoxic.

2.5. Experimental design

The effect of Fe(II) and H_2O_2 initial concentration on imidacloprid oxidation was assessed following the multivariate surface-response analysis described by Barros et al. [20]. Such technique is based on a central composite circumscribed design, consisting of a factorial design and star points. Variables were coded on two levels and normalised as unit values: +1 as the highest and −1 as the lowest value of a variable. Central points, coded as 0, were obtained from such extreme values and assayed in triplicate for statistical consistency. Star points were distributed at 1.414 distance from the central point.

The influence of Fe(II) and hydrogen peroxide initial concentrations in the range 15–35 mg L^{-1} and 150–400 mg L^{-1}, respectively, was assessed. Measured responses were: the time required to remove 80% imidacloprid (T_{80}), the time required to achieve total consumption of hydrogen peroxide (T_F) and total organic carbon removal yield. The latter is defined as

$$Y = \left(\frac{1 - \text{TOC}_{\text{residual}}}{\text{TOC}_{\text{initial}}}\right) \times 100 \quad (6)$$

The imidacloprid initial concentration (100 mg L^{-1}), temperature (25 °C) and initial pH (2.8) were kept as constant parameters. A total of 11 runs were conducted, and real and codified variables are presented in Table 1.

Data analysis, determination of empirical models and response surfaces, and optimisation were carried out using Modde 7.0™ commercial software. Statistical validation was determined by ANOVA test at 95% confidence level.

3. Results and discussions

3.1. Experimental design

Experimental results are summarised in Table 1. The treatment time to remove 80% of initial imidacloprid, depicted as T_{80}, ranges from 5 to 28 min, with greater T_{80} obtained at lower Fe(II)

initial concentrations. Hydrogen peroxide initial concentrations seem to present less influence on T_{80}. Since T_{80} is directly related to the rate of imidacloprid oxidation, such results would show that initial Fe(II) concentration have a much greater effect on the rate of free radical generation, than the initial peroxide concentration.

The time required to achieve total consumption of hydrogen peroxide (T_F) ranged from 38 to 145 min, under conditions tested here. T_F increases with the initial peroxide concentration, and tends to decrease as the Fe(II) concentration increases.

The reduction in total organic carbon (TOC) after all peroxide has been consumed (Y) varied between 9% and 77%, with greater values obtained at higher hydrogen peroxide initial doses. The extent of TOC reduction is less sensitive to Fe(II) concentration within the range tested here. TOC reduction is a direct measure of the extent of mineralization, which is highly dependent on the availability of oxidizing agents, in this case, hydrogen peroxide.

Polynomial quadratic models describing T_{80}, Y and T_F, as a function of initial hydrogen peroxide and iron concentrations are shown below, Eqs. (7)–(9), respectively. Model parameters were estimated from experimental values shown in Table 1, using least square multilinear regression analysis.

Corresponding model coefficients and confidence intervals (within brackets) are shown in the equations. Coded variables x_1 and x_2 correspond to H_2O_2 and Fe(II) initial concentrations, respectively. Corresponding parameters are normalised according to coded variables.

$$T_{80}(\text{min}) = 12.1(\pm1.7) + 1.2x_1(\pm1.4) - 7.1x_2(\pm1.0) + 2.2x_1^2(\pm1.5) + 2.0x_2^2(\pm1.3) \quad (7)$$

$$Y\,(\%) = 66.1(\pm2.8) + 22.8x_1(\pm2.0) - 5.0x_2(\pm2.0) - 11.7x_1^2(\pm2.1) - 4.4x_2^2(\pm2.1) + 3.5x_1x_2(\pm3.2) \quad (8)$$

$$T_F = 60(\pm3.7) + 33.9x_1(\pm2.2) - 17.6x_2(\pm2.2) + 19.1x_1^2(\pm2.7) + 6.8x_2^2(\pm2.7) \quad (9)$$

Multivariate linear regression correlation coefficients, R^2, for Eqs. (7)–(9) were 0.985, 0.997 and 0.998, respectively.

Contour plots calculated from these equations are illustrated in Figs. 3–5. As seen in Fig. 3, time to remove 80% imidacloprid decreases as the catalyst (Fe(II), x_2) concentration increases. On the other hand, the initial peroxide concentration (x_1) seems to have little effect on this response, particularly at low iron concentrations. As the iron concentration increases so does the sensitivity of the response to increases in hydrogen peroxide. This behaviour is reflected on the relatively low value of the x_1 linear coefficient in Eq. (7), and the statistically significant values of quadratic coefficients.

Fig. 4 shows that the extent of mineralization is greatly affected by the initial H_2O_2 concentration (x_1). Within the range of initial H_2O_2 concentrations used here (100–450 mg L^{-1}), the Fe(II) concentration (x_2) shows little effect on TOC reduction. Such poor influence could also be observed in Eq. (8), where x_2 and x_2^2 coefficients are negative and much smaller than the coefficient associated with H_2O_2 concentrations (x_1).

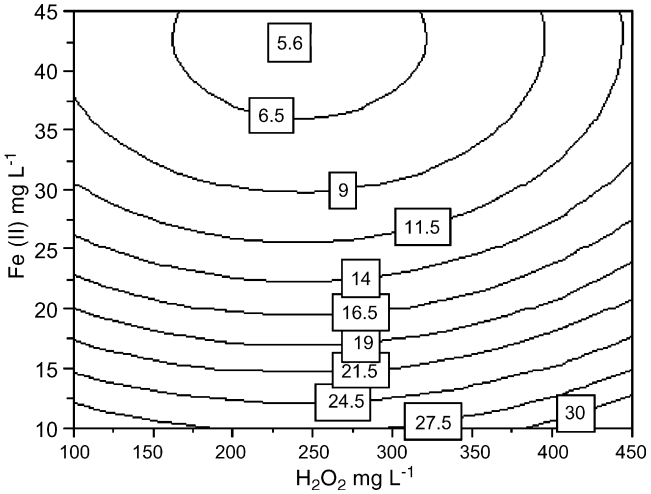

Fig. 3. Contour plot showing the time required to remove 80% of the imidacloprid by photo-Fenton reaction, as a function of initial Fe(II) and H_2O_2 concentrations.

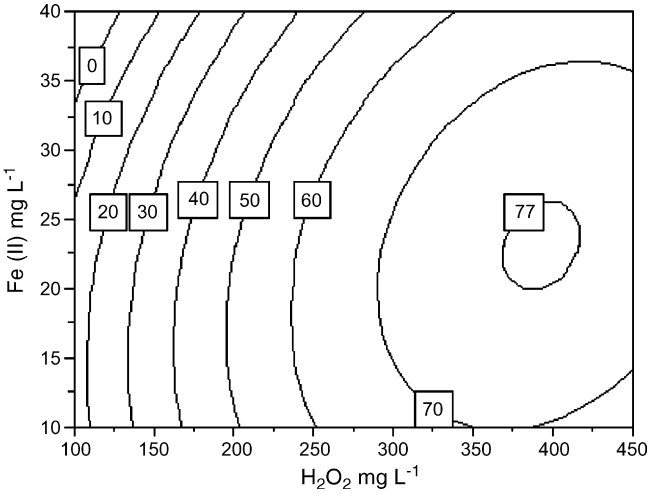

Fig. 4. Contour plot of the total organic carbon removal yield by photo-Fenton reaction, as a function of initial Fe(II) and H_2O_2 concentrations.

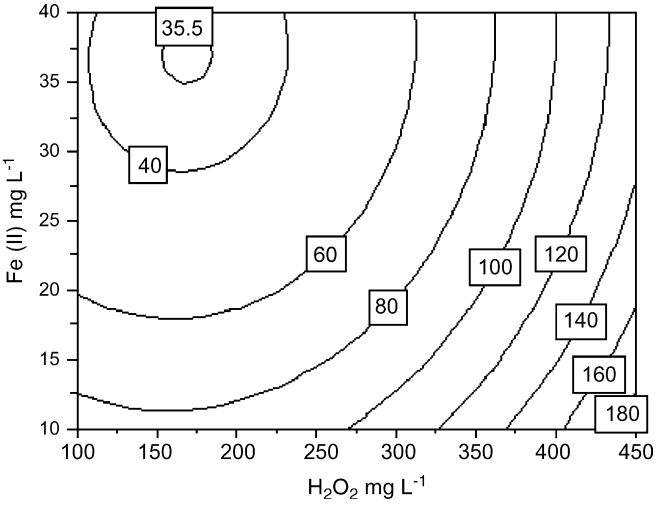

Fig. 5. Contour plot of the time required to achieve total consumption of H_2O_2 by photo-Fenton reaction, as a function of initial Fe(II) and H_2O_2 concentrations.

Fig. 5 shows that time (T_F) required for complete H_2O_2 consumption increases at higher H_2O_2 doses; moreover, T_F decreases as initial the Fe(II) concentration increases. The large positive values featured by x_1 and x_1^2 coefficients in Eq. (9), reflects such observations. However, at high Fe(II) concentrations T_F tends to increase, as depicted by the large negative x_2 quadratic coefficient in Eq. (9) (-6.8 ± 2.7).

According to other published studies, extreme values of H_2O_2 and/or Fe(II) concentrations seem to reduce the efficiency of organic pollutant removal [21,22]. Indeed, both H_2O_2 and Fe(II) could act as $HO^\bullet$ radical scavengers

$$Fe^{2+} + HO^\bullet \rightarrow Fe^{3+} + OH^- \quad (10)$$

$$H_2O_2 + HO^\bullet \rightarrow HO_2^\bullet + H_2O^\bullet \quad (11)$$

Such behaviour was not experimentally observed within the range of conditions used here.

According to model predictions, a minimum T_{80} around 5.5 min is obtained at 43 mg L^{-1} Fe(II) and 234 mg L^{-1} H_2O_2 initial concentrations. Moreover, maximum TOC reduction, around 77%, is obtained at 23 mg L^{-1} Fe(II) and 393 mg L^{-1} H_2O_2 initial concentrations. Finally, minimum overall process time 35 min could be obtained at 37 mg L^{-1} Fe(II) and 170 mg L^{-1} H_2O_2 initial concentrations. It could be concluded that high oxidant doses lead to greater extent of mineralization, but higher catalyst concentrations are required to increase the oxidation rate and reduce reaction times.

3.2. Imidacloprid degradation under selected conditions

A set of experiments at 35 mg L^{-1} Fe(II), and 150 and 350 mg L^{-1} H_2O_2 initial concentrations were conducted in order to validate model predictions and to assess the effect of those variables on process. Additionally, experiments were conducted using a mixture composed of 17.5 mg L^{-1} Fe(II) and 17.5 mg L^{-1} Fe(III), and 35 mg L^{-1} Fe(III), as initial source of iron. Runs using UV light in the absence of reagents, and combination of UV and H_2O_2 were also carried out in order to identify any possible effect on imidacloprid degradation. Fig. 6 summarises experimental results. Clearly, the contribution of photolysis and UV-H_2O_2 is rather negligible since no imidacloprid degradation was observed; under these conditions. These results could be explained by the fact that the experimental system used in this study features a negligible radiation fraction below 350 nm. It must be mentioned that H_2O_2 presents a maximum absorption peak at 220 nm.

Moreover, the initial imidacloprid degradation rate increases with the initial Fe(II) concentration. Interestingly, two distinctive kinetic regimes are observed in photo-Fenton runs containing Fe(II) as the initial iron source. Indeed, as seen in Fig. 6, there is a very fast, almost instantaneous, initial phase where nearly 50% of initial imidacloprid was degraded, followed by a slower phase featuring a monotonic oxidation until full degradation was achieved.

As shown in Fig. 7, Fe(II) undergoes a very fast oxidation to Fe(III), coinciding with the extensive imidacloprid initial degradation. Within the first few seconds, Fe(II) decreased to about

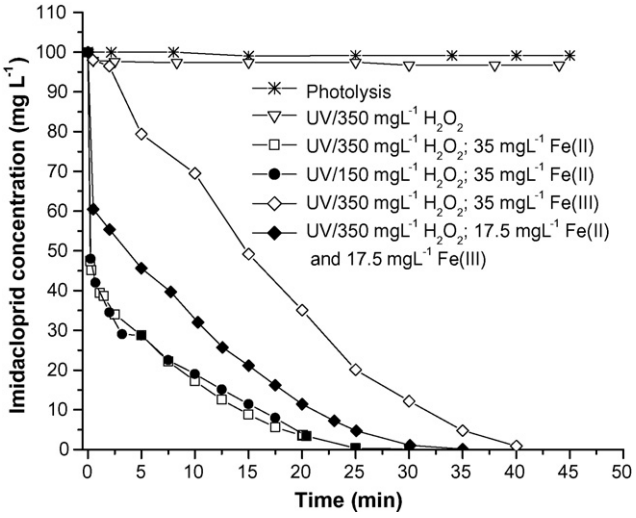

Fig. 6. Kinetic profile of imidacloprid solution degradation under different experimental conditions; pH = 2.8, $T = 25\,^\circ C$ and $I = 5 \times 10^{-6}$ Einstein s^{-1}.

10% of its initial value, and remained around that level for the rest of the experiment. Massive free radicals generated at that stage could account for such initial imidacloprid oxidation. This effect has not been reported in the literature to the extent seen in these experiments. The relatively large Fe(II) concentrations used here may have allowed to detect such behaviour.

Finally, when Fe(III) was used as the initial iron source, the initial imidacloprid oxidation rate was much slower than observed when Fe(II) was initially present, probably due to the fact that free radicals generation proceeded at slower rate, as Fe(III) was reduced to Fe(II). As observed in Fig. 7, the steady state Fe(II) concentration achieved during this run was similar to the level attained when Fe(II) was used as the initial iron source.

As predicted by the model, Fig. 6 show that H_2O_2 plays little role in the extent and rate of imidacloprid oxidation. Moreover, imidacloprid could be fully removed even at the low H_2O_2 condition tested here.

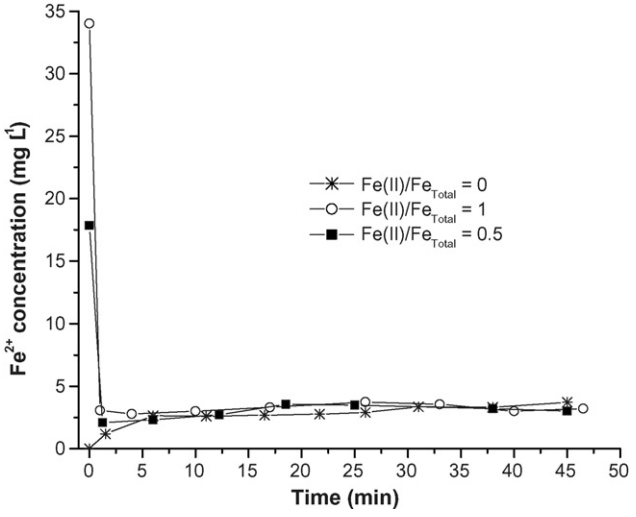

Fig. 7. Profile of Fe(II) concentration vs. the time of photo-Fenton reaction. Initial concentrations: 100 mg L^{-1} imidacloprid, 35 mg L^{-1} iron and 350 mg L^{-1} H_2O_2. pH = 2.8, $T = 25\,^\circ C$ and $I = 5 \times 10^{-6}$ Einstein s^{-1}.

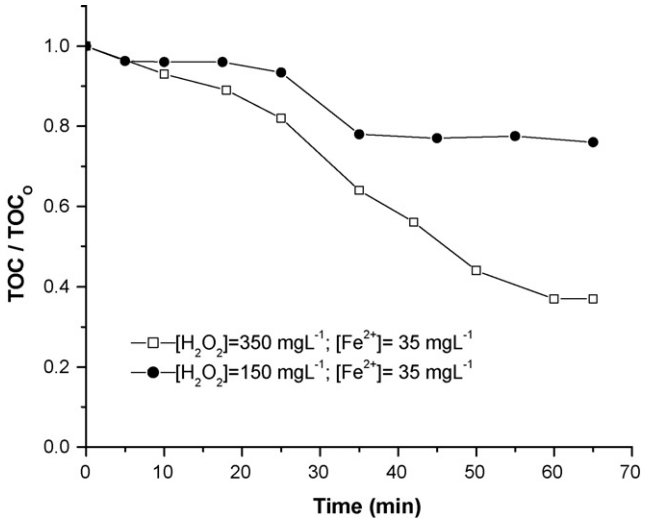

Fig. 8. TOC reduction for a 100 mg L^{-1} imidacloprid solution by photo-Fenton reaction at different H_2O_2 doses; pH = 2.8, T = 25 °C and $I = 5 \times 10^{-6}$ Einstein s^{-1}.

Figs. 8 and 9 show the extent of the oxidation process in the photo-Fenton system, in terms of TOC and COD reductions. At low H_2O_2 concentrations, the oxidation process was interrupted once H_2O_2 was fully consumed.

The average oxidation state (AOS) is a valuable parameter that can be used to estimate the oxidation extent of a complex solution consisting in the initial component and its oxidation products. The AOS of the reacting mixture was estimated according to Eq. (12) [23]. Where TOC and COD are expressed in mol of C L^{-1} and mol of O_2 L^{-1}, respectively.

$$\mathrm{AOS} = 4 \times \frac{\mathrm{TOC} - \mathrm{COD}}{\mathrm{TOC}} \quad (12)$$

The initial average oxidation state of the raw sample containing 100 mg L^{-1} imidacloprid commercial solution was 1.1. Under photo-Fenton treatment using 35 mg L^{-1} Fe(II) and 350 mg L^{-1} H_2O_2, the AOS increased almost linearly up to a value around 2.4 reached after 60 min treatment. Such average oxidation state is characteristic of highly oxidised short chain carboxylic acids, such as oxalic, acetic and formic acids [13,23]. On the other hand, when 150 mg L^{-1} H_2O_2 initial concentration was used a final AOS of 1.5 was reached, reflecting the low degree of mineralization attained. As stated before, a large extend of oxidation is obtained al high hydrogen peroxide concentrations.

3.3. Toxicity assessment

Bacillus subtilis and *Daphnia magna* were used to assess genotoxic and acute toxicities of samples treated by photo-Fenton, respectively. Tests were conducted using untreated 100 mg L^{-1} imidacloprid solution (E0), and after photo-Fenton treatment using 35 mg L^{-1} Fe(II) and 150 mg L^{-1} H_2O_2, for 40 min (E1); 35 mg L^{-1} Fe(II) and 400 mg L^{-1} H_2O_2, over 70 min (E2). Reaction times were set to allow full H_2O_2 consumption. After reaction was completed, pH was adjusted to 6.5 using NaOH 0.1 M before conducting toxicity tests. Fig. 10 and Table 2 summarise toxicity assessment results.

B. subtilis rec toxicity tests are used here as a preliminary assessment of any possible genotoxic effect in photo treated samples. Such test originally proposed by Mazza [19] provides a quantitative measure of any bacterial DNA damage due to the presence of genotoxic pollutants.

Fig. 10 shows experimental toxicity results from *B. subtillus* rec. It is seen that the 100 mg L^{-1} imidacloprid solution presents genotoxic effect since *B. subtilis* 1791,rec(−) N/N_0 is around 0.62, as compared with a value of around 1 in the case of *Bacillus subtilis* 1652, rec(+), corresponding to a plaque efficiency around 0.6. After 40 min treatment with 35 mg L^{-1} Fe(II) and 150 mg L^{-1} H_2O_2 the *B. subtilis* 1791, rec(−) N/N_0 ratio increases to 0.75, and *Bacillus subtilis* 1652, rec(+) maintains its N/N_0 around unity, with a plaque efficiency around 0.64. It must be pointed out that this sample has no imidacloprid left; therefore, intermediate oxidation by-products should account for

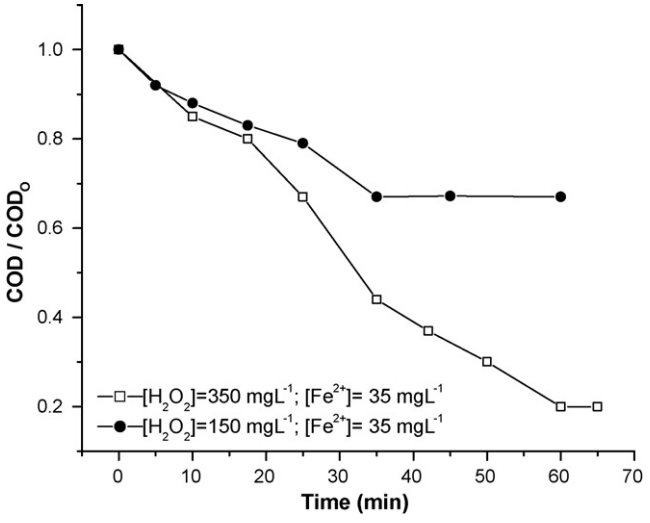

Fig. 9. COD removal in photo-Fenton treatment of imidacloprid solution as a function of H_2O_2 doses at pH = 2.8, T = 25 °C and $I = 5 \times 10^{-6}$ Einstein s^{-1}.

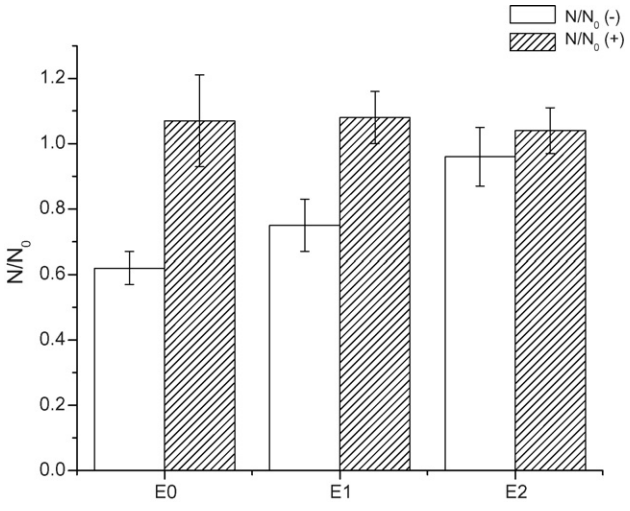

Fig. 10. Genotoxicity evolution of imidacloprid (E0) and oxidised samples at different mineralization stages (E1 and E2).

Table 2
Daphnia magna acute toxicity assays

Samples	Samples composition (mg L^{-1})			*Bacillus subtilis* genotoxicity	*Daphnia magna* acute toxicity	
	Imidacloprid	TOC	COD	Relative affinity, *A*	24 h LC_{50} (v/v%)	48 h LC_{50} (v/v%)
Untreated (E0)	100	70	110	0.58	40–70	10–20
E1	0	55	76	0.64	50–80	20–50
E2	0	20	6	0.93	ND	ND

Raw imidacloprid solution (E0) and samples treated by photo-Fenton: 35 mg L^{-1} Fe(II) and 150 mg L^{-1} H_2O_2 for 40 min (E1); 35 mg L^{-1} Fe(II) and 400 mg L^{-1} H_2O_2 for 70 min (E2). ND: not detected.

detected genotoxic effects. Finally, the sample treated by photo-Fenton treatment using 35 mg L^{-1} Fe(II) and 400 mg L^{-1} H_2O_2 for 70 min, showed a *B. subtilis* 1791,rec(−) N/N_0 ratio around 0.92, which is too low to be considered a genotoxic response. This sample features a relatively high degree of mineralization since more than 66% of original TOC was removed by treatment and the solution features an AOS over 2.5. It could be concluded that final by-products are highly oxidised and present no genotoxic activity towards *Bacillus subtilis*.

Acute toxicity was measured using *Daphnia magna*. Table 2 shows LC_{50} at 24 h and 48 h assays (i.e. percent sample volume in water dilution at which 50% lethality is observed after a set time).

As seen in the table, untreated imidacloprid samples (E0) present significant acute toxicity to Daphnia magna; with LC_{50} within 40–60% and 10–20%, after 24 h and 48 h culture, respectively. After partial photo-Fenton treatment (E1), 24 h and 48 h LC_{50} increase to 50–80% and 40–70%, respectively. It must be pointed out that imidacloprid was totally removed after such treatment, indicating that acute toxicity to Daphnia magna is due to the presence of partially oxidized intermediates.

Finally, samples treated for 70 min in the presence of 35 mg L^{-1} Fe(II) and 400 mg L^{-1} H_2O_2 (E2) presented no acute toxicity towards Daphnia magna.

4. Conclusions

Results reported above show that the surface-response methodology could be used to identify suitable operating conditions for effective imidacloprid removal by photo-Fenton processes.

The initial iron concentration plays a key role in the process kinetics whereas hydrogen peroxide concentration directly affects the extent of the oxidation process.

When Fe(II) was the initial iron source, imidacloprid degradation proceeds via two distinctive kinetics regimes: an initial stage of rapid imidacloprid reduction, followed by a slower oxidation process until complete removal. Initially, Fe(II) undergoes fast oxidation to Fe(III) leading to massive formation of free radicals and fast imidacloprid removal. Once iron oxidation–reduction reactions reach equilibrium, the contaminant oxidation rate slows down. When Fe(III) was the initial iron source, the free radical generation rate is much slower reducing the imidacloprid initial degradation rate.

Raw imidacloprid samples present significant acute toxicity to *Daphnia magna* and genotoxic effects on *Bacillus subtilis* sp. Such toxic effects remain detectable even after significant removal of the pesticide has been achieved, due to the presence of toxic by-products. Both acute toxicity and genotoxicity disappear after considerable mineralization resulting in final low molecular weight by-products. Theses results confirm the view that design and operation of photo-Fenton processes should focus on toxicity removal rather than on specific target pollutants.

Acknowledgements

This research was conducted with the financial support of Project Fondecyt N° 1060892.

References

[1] C. Cox, Imidacloprid: insecticide factsheet, J. Pest. Reform 21 (2001) 15–21.
[2] P.N. Moza, K. Hustert, E. Feicht, A. Kettrup, Photolysis of imidacloprid in aqueous solution, Chemosphere 36 (1998) 497–502.
[3] H. Wamhoff, V. Schneider, Photodegradation of imidacloprid, J. Agric. Food Chem. 47 (1999) 1730–1734.
[4] M. Lapertot, C. Pulgarín, P. Fernández-Ibáñez, M.I. Maldonado, L. Pérez-Estrada, P. Oller, W. Gernjak, S. Malato, Enhancing biodegradability of priority substances (pesticides) by solar photo-Fenton, Water Res. 40 (2006) 1086–1094.
[5] I. Oller, W. Gernjak, M.I. Maldonado, L.A. Pérez-Estrada, J.A. Sánchez-Pérez, S. Malato, Solar photocatalytic degradation of some hazardous water-soluble pesticides at pilot-plant scale, J. Hazard. Mat. B138 (2006) 507–517.
[6] S. Chiron, A. Fernández-Alba, A. Rodriguez, E. García-Calvo, Pesticide chemical oxidation: state-of-the-art, Water Res. 34 (2000) 366–377.
[7] S. Malato, J. Blanco, J. Cáceres, A.R. Fernández-Alba, A. Agüera, A. Rodríguez, Photocatalytic treatment of water-soluble pesticides by photo-Fenton and TiO_2 using solar energy, Catal. Today 76 (2002) 209–220.
[8] A.R. Fernández-Alba, D. Hernando, A. Agüera, J. Cáceres, S. Malato, Toxicity assays: a way for evaluating AOPs efficiency, Water Res. 36 (2002) 4255–4262.
[9] C.W. Paterlini, F.P. Nogueira, Multivariate analysis of photo-Fenton degradation of the herbicides tebuthiuron, diuron and 2,4-D, Chemosphere 58 (2005) 1107–1116.
[10] F. Haber, J. Weiss, The catalytic decomposition of hydrogen peroxide by iron salts, Proc. Roy. Soc. A 134 (1934) 332–351.
[11] J. De Laat, H. Gallard, Catalytic decomposition of hydrogen aqueous solution: mechanism and kinetic modeling, Environ. Sci. Technol. 33 (1999) 2726–2732.
[12] J.J. Pignatello, Dark and photoassisted Fe^{3+}-catalyzed degradation of chlorophenoxy herbicides by hydrogen peroxide, Environ. Sci. Technol. 26 (1992) 944–951.
[13] S. Malato, J. Cáceres, A. Agüera, M. Mezcua, D. Hernando, J. Vial, A.R. Fernández-Alba, Degradation of imidacloprid in water by photo-Fenton and TiO_2 photocatalysis at a solar pilot plant: a comparative study, Environ. Sci. Technol. 35 (2001) 4359–4366.

[14] J. Marugán, M.J. López-Muñoz, W. Gernjak, S. Malato, Fe/TiO_2/pH interactions in solar degradation of imidacloprid with TiO_2/SiO_2 photocatalysts at pilot-plant scale, Ind. Eng. Chem. Res. 45 (2006) 8900–8908.
[15] S.L. Murov, Handbook of Photochemistry, Marcel Dekke, Inc., New York, 1973.
[16] APHA-AWWA-WPCF, Métodos normalizados para análisis de aguas potables y residuales, 17nd ed., Díaz Santos S.A, Madrid, España, 1992.
[17] NCh 2083 Of Bioensayos de toxicidad aguda mediante la determinación de la inhibición de la movilidad de Daphnia magna o Daphnia pulex (Crustacea, Cladocera), 1999.
[18] USEPA, Methods for measuring the acute toxicity of effluents and receiving water of freshwater and marine organisms, USEPA/600/4-90/027F, 1991.
[19] G. Mazza, *Bacillus subtilis* "rec assay" test with isogenic strains, Appl. Environ. Microbiol. 43 (1982) 177–184.
[20] B. Barros, I.S. Scarminio, R.E. Bruns, Como fazer experimentos. Pesquisa e desenvolvimento na ciência e na indústria, Editora da UNICAP, Campinas, 2001.
[21] M. Pera-Titus, V. García-Molina, M.A. Baños, J. Giménez, S. Esplugas, Degradation of chlorophenols by means of advanced oxidation processes: a general review, Appl. Catal. B: Environ. 47 (2004) 219–256.
[22] F. Torrades, M. Pérez, H.D. Mansilla, J. Peral, Experimental design of Fenton and photo-Fenton reactions for the treatment of cellulose bleaching effluents, Chemosphere 53 (2003) 1211–1220.
[23] W. Stumm, J.J. Morgan, Aquatic Chemistry, second ed., Wiley, New York, 1991.